

THE EFFECTS OF GLASS DOPING, TEMPERATURE AND TIME ON THE MORPHOLOGY, COMPOSITION, AND IRON REDOX OF SPINEL CRYSTALS

J. Matyáš¹, J. E. Amonette¹, R. K. Kukkadapu¹, D. Schreiber¹, A. A. Kruger²

1. Pacific Northwest National Laboratory

Richland, WA, USA

2. Office of River Protection

Richland, WA, USA

ABSTRACT

Precipitation of large crystals/agglomerates of spinel and their accumulation in the pour spout riser of a Joule-heated ceramic melter during idling can plug the melter and prevent pouring of molten glass into canisters. Thus, there is a need to understand the effects of spinel-forming components, temperature, and time on the growth of crystals in connection with an accumulation rate. In our study, crystals of spinel $[\text{Fe}, \text{Ni}, \text{Mn}, \text{Zn}, \text{Sn}][\text{Fe}, \text{Cr}]_2\text{O}_4$ were precipitated from simulated high-level waste borosilicate glasses containing different concentrations of Ni, Fe, and Cr by heat treating at 850 and 900°C for different times. These crystals were extracted from the glasses and analyzed with scanning electron microscopy and image analysis for size and shape, with inductively coupled plasma–atomic emission spectroscopy and atom probe tomography for concentration of spinel-forming components, and with wet colorimetry and Mössbauer spectroscopy for $\text{Fe}^{2+}/\text{Fe}_{\text{total}}$ ratio. High concentrations of Ni, Fe, and Cr in glasses resulted in the precipitation of crystals larger than 100 μm in just two days. Crystals were a solid solution of NiFe_2O_4 , NiCr_2O_4 , and $\gamma\text{-Fe}_2\text{O}_3$ (identified only in the high-Ni-Fe glass) and also contained small concentrations of less than 1 at% of Li, Mg, Mn, and Al.

INTRODUCTION

The U.S. Department of Energy is building the Waste Treatment and Immobilization Plant at the Hanford Site in Washington State to remediate 55 million gallons of radioactive waste that is being temporarily stored in 177 underground tanks. The plan is to vitrify the waste into a durable borosilicate glass with Joule-heated ceramic melters. To do this efficiently and cost-effectively, the waste loading in the glasses must be maximized.¹ The major factor limiting waste loading in Hanford high-level waste (HLW) glasses is the precipitation, growth, and subsequent accumulation of spinel crystals $[\text{Fe}, \text{Ni}, \text{Mn}, \text{Zn}, \text{Sn}][\text{Fe}, \text{Cr}]_2\text{O}_4$ in the glass discharge riser of the melter during idling.^{2,3} These crystals can reach a size of a few hundreds of micrometers and because of their high density ($\sim 5.3 \times 10^3 \text{ kg/m}^3$) settle down fast, forming a thick sludge layer that prevents the discharge of the molten glass into stainless steel canisters.

Spinel crystals have a crystal structure of the natural spinel MgAl_2O_4 and can be described as a cubic close-packed arrangement of oxygen atoms with divalent and trivalent cations at two different crystallographic sites. These sites have tetrahedral and octahedral oxygen coordination. A remarkable feature of spinel structure is that it is able to form a virtually unlimited number of solid solutions. This means that the composition of spinel can be varied significantly without altering the basic crystalline structure. Depending on cation distribution, a spinel can be normal, inverse, or mixed. In a normal spinel (e.g., NiCr_2O_4 and ZnFe_2O_4) the tetrahedral and octahedral sites are occupied by divalent and trivalent cations, respectively. If tetrahedral sites are completely occupied by trivalent cations and the octahedral sites are shared by both divalent and trivalent cations, it is an inverse spinel (e.g., NiFe_2O_4 and $\gamma\text{-Fe}_2\text{O}_3$). However, most spinels are mixed spinels (e.g. MnFe_2O_4) in which divalent and trivalent cations occupy both tetrahedral and octahedral sites.

This paper focuses on investigating the effects of temperature, time, and glass doping with metal oxides on the morphology, composition, and iron redox of spinel crystals in the HLW borosilicate glasses in connection with crystal accumulation in the riser of the melter. Crystals of spinel were precipitated from glasses containing different concentrations of Ni, Fe, and Cr by heat treating at 850 or 900°C for different times. These crystals were then recovered and analyzed with scanning electron microscopy (SEM) and image analysis for size and shape, with inductively coupled plasma atomic emission spectroscopy (ICP-AES) and atom probe tomography (APT) for concentration of spinel-forming components, and with wet colorimetry and Mössbauer spectroscopy for $\text{Fe}^{2+}/\text{Fe}_{\text{total}}$ ratio.

The following sections describe the experimental approach and the results obtained from analysis of crystals with an array of instrumentation.

MATERIALS

Three glasses were formulated from previously used baseline glass² by varying component fractions of NiO, Fe₂O₃, and Cr₂O₃. The remaining components were kept in the same proportions as in the baseline glass. Table 1 shows the compositions of tested glasses (Ni1.5, Ni1.5/Fe17.5, Ni1.5/Cr0.3) in mass fraction of oxides and halogens. Glasses were prepared from AZ-101 simulant⁴ and additives (H₃BO₃, Li₂CO₃, Na₂CO₃, SiO₂, Cr₂O₃, NiO, and Fe₂O₃). These components were hand-mixed in a plastic bag, mixed in an agate mill for 5 min, and melted at 1200°C for an hour in a Pt-10%Rh crucible. The glass melt was quenched, ground in a tungsten carbide mill for 2 min, and remelted at the same temperature for the same time before being poured into double crucible assemblies² that were placed inside the furnace at 850 or 900°C. The double crucibles were removed at various times and cross-sectioned. To extract crystals from glasses, accumulated layers were cut out from the bottoms of crucibles and treated with heated (60°C) 20% HNO₃ overnight to dissolve the glass, and then with 5% HF to dissolve the residual silica gel.

Table 1. Glass compositions in mass fraction of oxides and halogens.^a

Component	Ni1.5	Ni1.5/Fe17.5	Ni1.5/Cr0.3
Al ₂ O ₃	0.0814	0.0784	0.0813
B ₂ O ₃	0.0792	0.0763	0.0791
CaO	0.0057	0.0054	0.0057
CdO	0.0064	0.0062	0.0064
Cr ₂ O ₃	0.0017	0.0016	0.0030
Fe ₂ O ₃	0.1438	0.1750	0.1436
K ₂ O	0.0034	0.0032	0.0034
Li ₂ O	0.0197	0.0190	0.0197
MgO	0.0013	0.0012	0.0013
MnO	0.0035	0.0033	0.0035
Na ₂ O	0.1850	0.1781	0.1848
NiO	0.0150	0.0150	0.0150
P ₂ O ₅	0.0032	0.0031	0.0032
SiO ₂	0.3995	0.3847	0.3989
ZrO ₂	0.0412	0.0397	0.0411
Ce ₂ O ₃	0.0020	0.0019	0.0020

^a Each glass contained 0.0009 BaO, 0.0002 Cl, 0.0001 CoO, 0.0004 CuO, 0.0001 F, 0.0022 La₂O₃, 0.0018 Nd₂O₃, 0.0010 SnO₂, 0.0008 SO₃, 0.0003 TiO₂, 0.0002 ZnO.

METHODS

Whole Rock Analysis

Crystals were dissolved using lithium metaborate/tetraborate fusions, and solutions were analyzed with ICP-AES. Two solid standards, National Institute of Standards and Technology (NIST) Standard Reference Material (SRM) 278 Obsidian Rock and NIST SRM Basalt Rock, were run with samples to validate the analysis. The recoveries for analytes were in the range from 95 to 105%, except for Ba (78%), K (77%), Zr (80%), and Na (92%). Duplicates, which were used to assess the precision of the preparation process, showed a good agreement for analytes, with relative percent difference of less than 9%.

Atom Probe Tomography

Crystals collected from high-Ni-Fe glass (Ni_{1.5}/Fe_{17.5}-900°C-7D) were dispersed onto a carbon tape and coated with chromium. A wedge-shaped bar ($25 \times 3 \times 2 \mu\text{m}$) was extracted from a (111) facet of the selected crystal surface with a focused ion beam liftout method. Eight specimens with an apex diameter of 80 to 120 nm were prepared and analyzed with a Leap 4000X HRTM 3D Atom Probe Microscope (CAMECA, Gennevilliers, France) in laser pulsing mode. Figure 1 shows SEM images of a crystal with a wedge-shaped bar region extracted and a conical specimen for analysis with APT. The specimen temperature and evaporation rate were fixed at 40 K and 2.5×10^{-3} ions per pulse, respectively. The laser energy was 32 pJ per pulse.

Atom probe tomography provided a three-dimensional (3-D) elemental map and chemical identity of about 60% of the atoms in the analysis volume with a spatial resolution of ~ 0.1 nm. Since its detection efficiency is independent of atomic number it was also used to detect and quantify Li.

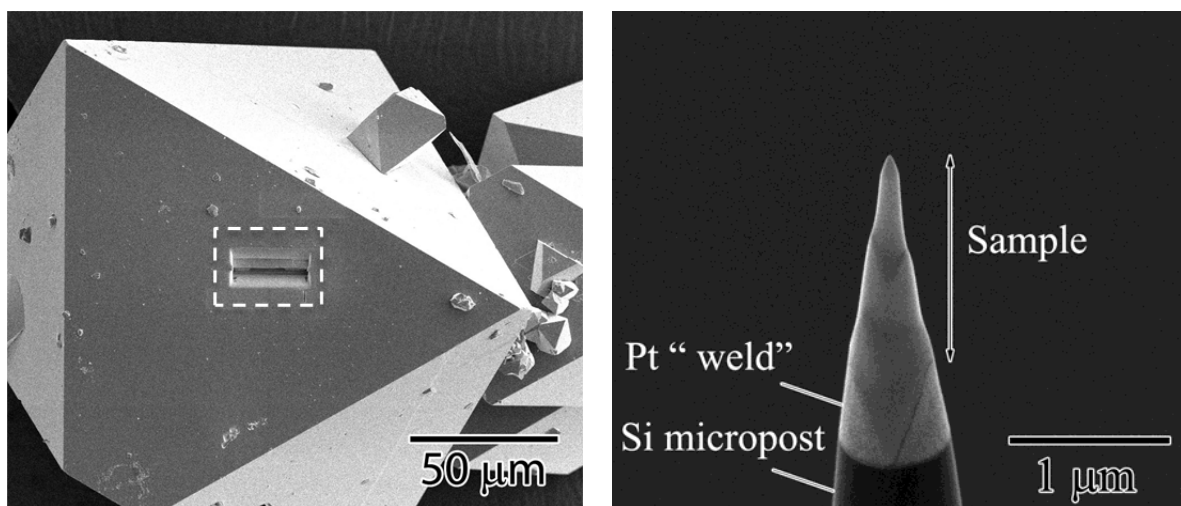


Figure 1. SEM images of spinel crystal (Ni_{1.5}/Fe_{17.5}-900°C-7D) showing the wedge-shaped region removed for preparation of a specimen (dashed line rectangle) and a conical specimen for APT analysis.

Scanning Electron Microscopy and Image Analysis

Crystals were sprinkled onto a carbon tape, sputter-coated with Au/Pd and analyzed for morphology with a JEOL JSM-5900 SEM (SEMTech Solutions Inc., North Billerica, Massachusetts). The microscope was set up at accelerating voltage 15 kV, spot size 42-45, and working distance 12 mm. Clemex Vision PE 6.0 image analysis software (Clemex Technologies Inc., Longueuil, Canada) was used to measure the length of the edge of 50 crystals for each glass composition.

Wet Colorimetry

For each sample, approximately 15 mg of crystals were gently ground with a sapphire mortar and pestle under acetone. The nitrogen-dried powders were converted into solutions by treating with 6 mL of 48% HF at 94°C for 48 h. The solutions were then neutralized with a N₂-sparged cocktail containing 12 mL of 10% H₂SO₄, 60 mL of 5% H₃BO₃, 2 mL of a solution of 200 mg of 1,10-phenanthroline in 95% ethanol, and 35 mL of deionized water. Phenanthroline was added to complex Fe²⁺ and thereby prevent its oxidation. To determine the quantity of Fe²⁺, 1 ml of neutralized digestate was mixed with 10 mL of 1% sodium citrate. To determine the quantity of Fe_{total}, 1 ml of neutralized digestate was mixed with 10 ml of a solution containing 1% sodium citrate and 1% NH₂OH·H₂SO₄. After the minimum equilibration time of 90 min, the absorptivities of the Fe²⁺ and the Fe_{total} were determined at a wavelength of 510 nm with a Shimadzu UV-2401 PC UV-VIS spectrophotometer (Shimadzu, Columbia, Maryland).

Several control and standard samples were run with experimental samples. These included an iron-free reagent blank, ferrous diammonium sulfate hexahydrate (FAS, Sigma F-1543, Lot # 58H0465, nominal purity 101.3%), hematite (Fe₂O₃, Alfa Aesar 14680, Lot # G21U020, nominally 99.945% pure on metals basis), and magnetite (Fe₃O₄, Sigma-Aldrich 518158, Lot # MKBJ5645V, nominal Fe content 71.8% vs. 72.36% stoichiometric).

⁵⁷Fe Mössbauer Spectroscopy

Mössbauer analysis was performed on crystals collected from Ni1.5, Ni1.5/Fe17.5, and Ni1.5/Cr03 glasses which were heat-treated at 900°C for 7 days. Approximately 20-50 mg of crystals per sample was mixed with petroleum jelly in a cylindrical holder with inside diameter 1.27 cm and height 0.94 cm. The completely filled holders were sealed at both ends with Kapton tape, which was then snapped into the holders with carbonized polyethyletherketone rings to ensure tightness.

Mössbauer spectra were collected at room temperature and 10 K with WissEL Elektronik (Starnberg, Germany) or Web Research Company (St. Paul, MN) instruments, which included an SHI-850 closed-cycle cryostat (Janis Research Company, Inc., Wilmington, MA), a CKW-21 helium compressor unit (Sumitomo Cryogenics of America, Chicago, IL), and an Ar-Kr proportional counter detector (WissEL) or Ritvec (St. Petersburg, Russia) NaI detection system (Web Research Company). A ⁵⁷Co/Rh source (Ritvec, Russia) with 50-75 mCi initial strength was used as the gamma energy source. The velocity transducers were operated in a constant acceleration mode (23 Hz, ±12 mm/s). The transmitted counts were stored in a multichannel scalar as a function of energy (transducer velocity) using a 1024-channel analyzer. The data were folded to 512 channels to provide a flat background and a zero-velocity position corresponding to the center shift of 25-μm-thick α-Fe foil (Amersham, Amersham, England) at room temperature. The Mössbauer data were modeled with Recoil software (University of Ottawa, Ottawa, Canada) using a Voight-based structural fitting routine.⁵

RESULTS AND DISCUSSION

The whole rock analysis revealed that the concentrations of major spinel-forming components Ni, Fe, and Cr varied with glass composition, temperature, and time. The concentration of Fe ranged from 0.7 to 0.8 mol, Ni from 0.3 to 0.4 mol, and Cr from 0.02 to 0.1 mol. Figure 2 illustrates the changes in concentration of Ni, Fe, and Cr over time for different glass compositions and temperatures. Adding more Ni, Fe, and Cr to glasses resulted in increased concentrations of these components in the crystals. Analysis also identified the presence of other spinel-forming components such as Mn, Al, and Mg in concentrations of less than 0.01 mol.

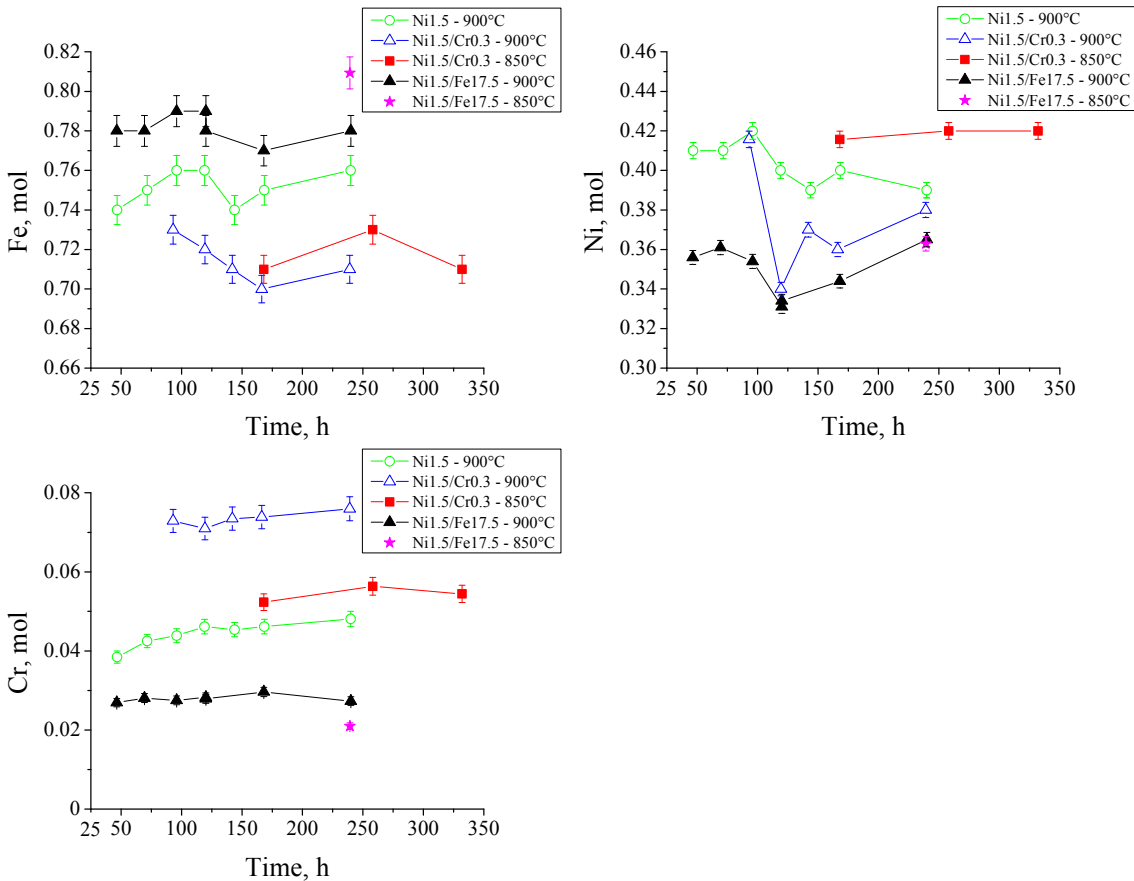


Figure 2. Effect of glass composition, temperature, and time on concentration of Fe, Ni, and Cr in spinel crystals.

A 3-D reconstructed volume $\sim 60 \times 60 \times 140 \text{ nm}^3$ of 10 million atoms was obtained for the cone-shaped specimen prepared from spinel crystal that precipitated from high-Ni-Fe glass. Figure 3 shows concentration profiles of Ni, Fe, and Cr along the z-axis from top to bottom. The measured concentrations were about constant over the depth of 140 nm, suggesting non-existence of short-range composition fluctuations within the reconstructed volume. Observed small-scale fluctuations in concentrations were most likely the result of occasional laser scans during data acquisition, which were performed to maintain the laser alignment on the specimen. Table 2 shows minimum, maximum, and average concentrations of different elements in at% within the reconstructed volume. Good agreement with chemical analysis was obtained for average concentrations of Ni (30.2 vs. 31.6 at%) and Fe (14.5 vs. 14.0 at%). However, the average concentration of Cr from chemical analysis was 1.2 at% compared to 2.1 at% from APT. This suggests formation of more NiCr_2O_4 at the late stage of crystal growth and possible long-range composition fluctuations. This needs to be confirmed, however, by APT analysis of additional specimens from the interior of the crystal. The analysis also revealed the presence of other spinel-forming components such as Li, Mg, Mn, and Al, which were detected in small concentrations up to 0.9 At%, providing evidence that these components participate in the formation of spinel solid solution in the HLW glasses.

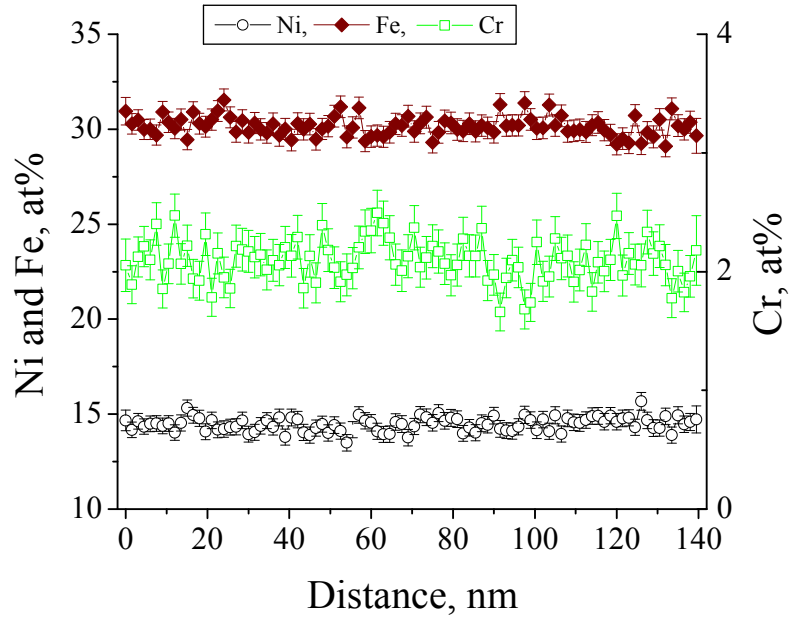


Figure 3. Concentration profiles of Ni, Fe, and Cr along the z-axis of the specimen (from top to bottom), including error bars.

Table 2. Minimum, maximum, and average concentrations of different elements in at% within the reconstructed volume.

	Ni	Fe	Cr	O	Li	Mg	Mn	Al
Min.	13.5	29.1	1.7	50.3	0.4	0	0.2	0
Max.	15.7	31.5	2.5	53.6	0.9	0.2	0.4	0.3
Avg.	14.5	30.2	2.1	51.7	0.7	0.1	0.3	0.2

Figure 4 shows the morphology of crystals precipitated from different glass compositions after 2 and 7 days at 900°C. Single octahedral crystals as well as aggregates of two or more intergrown individual crystals were observed. The average size of crystals was greater than 90 μm after only two days at 900°C. In addition, the size of crystals did not change much between 2 and 7 days for the same glass composition. This suggests a rapid growing period early in the test and indicates that frequent occurrence of melter idling periods 1-2 days long may result in thick layers, which can eventually prevent pouring of molten glass. Adding Cr and Fe to high-Ni glass significantly increased the average crystal size from ~90 to ~150 μm. Considering that the Stokes settling velocity is proportional to the square of the particle effective radius, the 150-μm crystals would settle ~2.8 times faster than the 90-μm crystals. This substantial increase in the rate of settling can considerably shorten the lifetime of the melter.

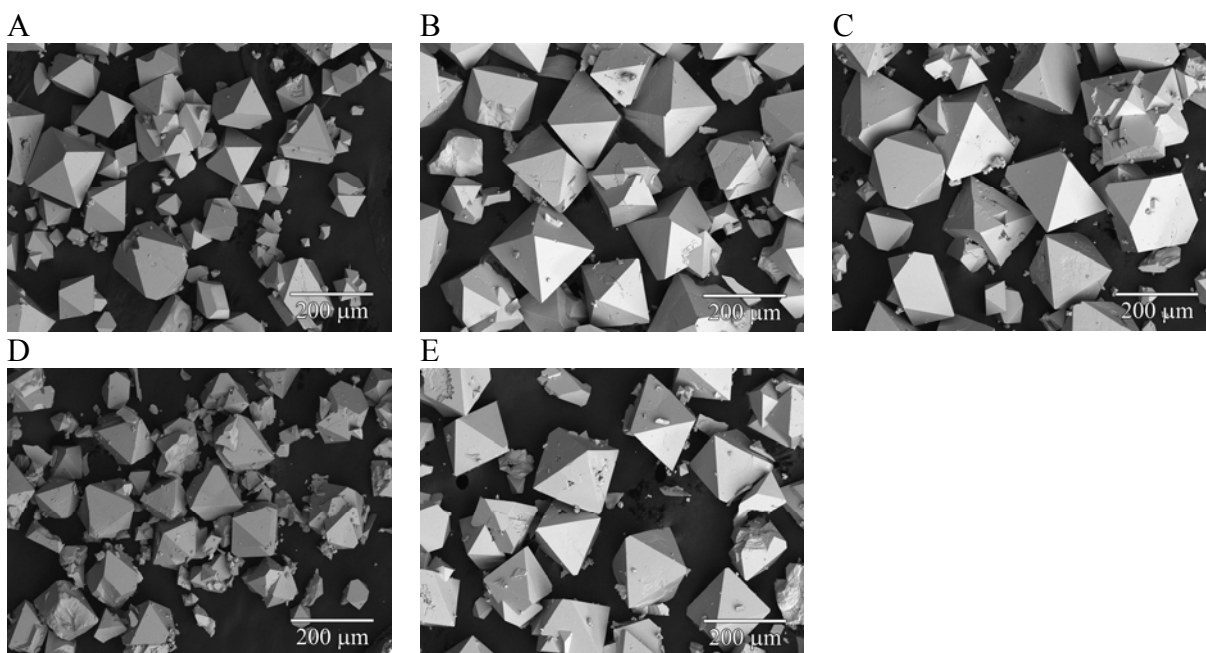


Figure 4. SEM images of crystals precipitated from different glasses at 900°C at different times, including average crystal size (h): A) Ni1.5 – 7 days, $h = 92.4 \pm 28.2 \mu\text{m}$; B) Ni1.5/Cr0.3 – 7 days, $h = 151.1 \pm 23.2 \mu\text{m}$; C) Ni1.5/Fe17.5 – 7 days, $h = 148.9 \pm 35.9 \mu\text{m}$; D) Ni1.5 – 2 days, $h = 93.9 \pm 18.3 \mu\text{m}$; and E) Ni.5/Fe17.5 – 2 days, $h = 140.9 \pm 16.2 \mu\text{m}$.

Table 3 shows iron redox of crystals as determined by wet colorimetry. Crystals contained 37.1-45.2 mass% iron, including 0.4-0.5 mass% Fe^{2+} . These values correspond to $\text{Fe}^{2+}/\text{Fe}_{\text{total}}$ ratios from 0.9 to 1%. The homogeneous low concentrations of Fe^{2+} suggest that the iron redox equilibrium in crystals was established quickly and remained constant over time. Table 3 also provides comparison for the measured total iron concentrations from wet colorimetry and chemical analysis. Good agreement was obtained for 18 samples, exhibiting relative standard deviations (RSD) of less than 3%. The remaining four samples (numbers in bold letters in the Table 3) showed higher but still acceptable RSD in the range from 6 to 10%.

Table 4 compares measured and target concentrations of Fe^{2+} , Fe^{3+} , and $\text{Fe}^{2+}/\text{Fe}_{\text{total}}$ for FAS, Fe_3O_4 , and Fe_2O_3 . Consistent results were obtained for the standard FAS sample. A total iron close to theoretical value and a small amount of ferrous iron (~ 0.5 mass%) were present in the hematite control sample. However, the magnetite seemed to be oxidized by about 17%. This can be explained by the high susceptibility of nanoparticles to oxidation during the preparation of solutions for analysis.

The Mössbauer spectroscopic method validated iron redox results from wet colorimetry and also provided some insight on distribution of iron cations within spinel structure. Ferrous quadrupole split doublets were not present in the spectrums of samples, indicating absence of Fe^{2+} in the crystals. Fig 5 shows an example of Mössbauer spectra for crystals extracted from Ni1.5/Cr0.3 glass. Modeled spectral areas of tetrahedral (Td) 1 and 2, and octahedral sites (Oh) were 20.5 ± 2.8 , 36.6 ± 2.7 , and $42.8 \pm 2.2\%$, respectively. Spectral features and relative areas for Td and Oh sites were similar to trevorite in which a small fraction of Fe^{3+} in Oh sites was substituted with Cr^{3+} .

Figure 6 shows a plot of the sum of concentrations of Fe and Cr as a function of time for different glass compositions and two temperatures. This plot was made by normalizing concentrations of Fe and Cr to 1 mol of Ni, and considering that all the iron in the crystals is in

the form of Fe^{3+} . Spinel crystals precipitated from high-Ni (Ni1.5) and high-Ni-Cr (Ni1.5/Cr0.3) glasses were a solid solution of trevorite (NiFe_2O_4) and nichromite (NiCr_2O_4). Adding more iron to high-Ni glass (Ni1.5/Fe17.5) resulted in the formation of NiFe_2O_4 and NiCr_2O_4 , and maghemite ($\gamma\text{-Fe}_2\text{O}_3$), which was confirmed by X-ray diffraction analysis.

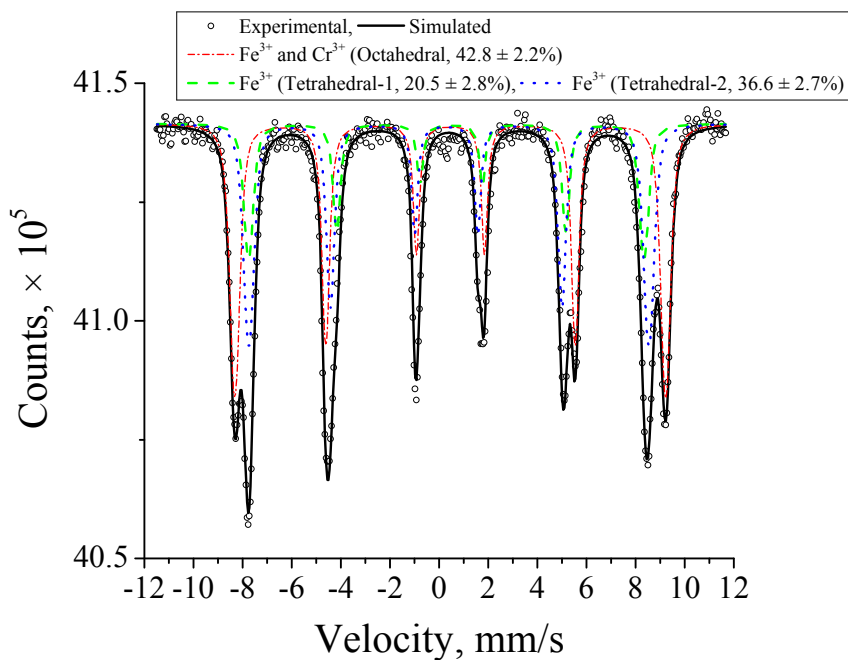
Table 3. Iron redox of crystals from wet colorimetry.

Glass	Temperature, °C	Time, days	Fe^{2+} , mass%	$\text{Fe}_{\text{total}}^{\text{a}}$, mass%	$\text{Fe}^{2+}/\text{Fe}_{\text{total}}$, %
Ni1.5	900	2	0.4	40.7 (41.6)	0.98
		3	0.4	40.5 (41.8)	0.99
		4	0.4	40.9 (42.5)	0.98
		5	0.4	41.7 (42.5)	0.96
		6	0.4	42.3 (41.4)	0.95
		8	0.4	41.1 (42.0)	0.97
		10	0.4	38.5 (42.1)	1.04
Ni1.5/Cr0.3	900	4	0.4	40.1 (40.5)	1.00
		5	0.4	40.2 (40.2)	1.00
		6	0.4	37.1 (39.8)	1.08
		7	0.4	38.9 (39.3)	1.03
		10	0.4	39.0 (39.7)	1.03
Ni1.5/Fe17.5	900	2	0.4	43.7 (43.5)	0.92
		3	0.4	42.9 (43.9)	0.93
		4	0.5	44.4 (43.9)	1.13
		5	0.4	44.0 (43.3)	0.91
		7	0.4	40.0 (43.3)	1.00
		10	0.4	44.9 (43.5)	0.89
Ni1.5/Cr0.3	850	7	0.4	40.7 (39.9)	0.98
		11	0.4	38.2 (40.7)	1.05
		14	0.4	39.4 (39.9)	1.02
Ni1.5/Fe17.5	850	10	0.4	45.2 (45.2)	0.88

^a Fe_{total} values in brackets were obtained from chemical analysis.

Table 4. Measured and target values (in brackets) of iron redox for standard and controlled samples from wet colorimetry measurements.

	Fe^{2+} , mass%	Fe^{3+} , mass%	$\text{Fe}^{2+}/\text{Fe}_{\text{total}}$, %
FAS	14.5 ± 0.8 (14.4)	0.5 ± 0.4 (0)	96.67 ± 0.4 (100)
Fe_3O_4	19.8 ± 0.7 (23.9)	54.5 ± 0.1 (47.9)	26.68 ± 0.8 (33.3)
Fe_2O_3	0.5 ± 0.0 (0)	70.1 ± 0.3 (69.9)	0.71 ± 0.3 (0)



4.5

Figure 5. Mössbauer spectrum at 10 K for crystals extracted from Ni_{1.5}/Cr_{0.3} glass heat-treated at 900°C for 7 days.

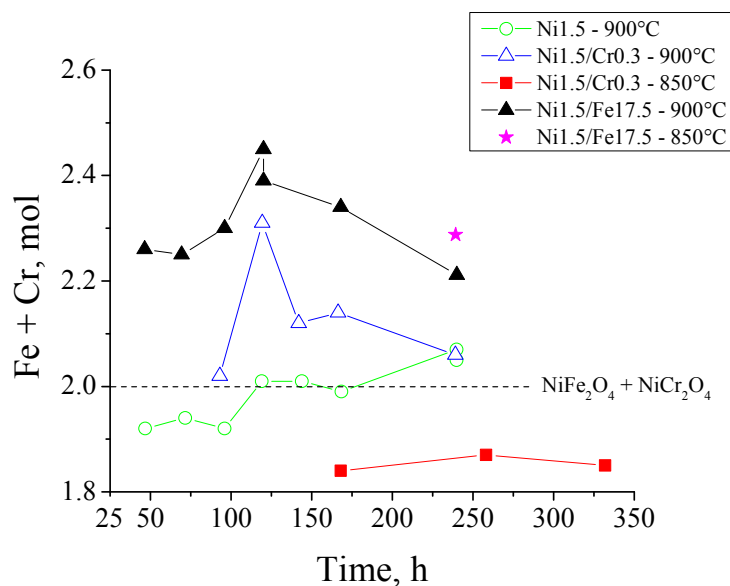


Figure 6. Sum of concentrations of Fe and Cr normalized to 1 mol of Ni for crystals extracted from glasses heat-treated at 850 and 900°C for different time periods.

CONCLUSIONS

This one-of-a-kind study on crystals extracted from simulated HLW glasses clearly shows the effects of spinel-forming components (Ni, Fe, and Cr) temperature, and time on crystal growth. Glasses containing high concentrations of Ni, Fe, and Cr were susceptible to precipitation of crystals larger than 100 μm in just two days. This would result in excessive settling in the riser of the melter and potential plugging even for frequent short-term idling periods. Interestingly, redox measurements of crystals with wet colorimetry and Mössbauer spectroscopy revealed that more than 99% of the total iron is in the form of Fe^{3+} , indicating

absence of magnetite. Major components of spinel solid solution for crystals extracted from the high-Ni and high-Ni-Cr glasses were NiFe_2O_4 and NiCr_2O_4 . However, besides these phases, $\gamma\text{-Fe}_2\text{O}_3$ was present in the spinel solid solution of crystals from high-Ni-Fe glass. Chemical analysis and APT confirmed that Li, Mg, Mn, and Al are also present in the spinel structure in the small concentrations of less than 1 at%.

ACKNOWLEDGMENT

This project has been supported by the U. S. Department of Energy's Waste Treatment and Immobilization Plant Federal Project Office under the direction of Dr. Albert A. Kruger. Authors acknowledge the support of Environmental Molecular Sciences Laboratory under proposal 48118 to analyze crystals of spinel with Mössbauer spectroscopy. Pacific Northwest National laboratory is operated by Battelle for the U.S. Department of Energy under Contract DE-AC0576RL01830.

REFERENCES

- ¹J. D. Vienna, D. S. Kim, D. C. Skorski, and J. Matyáš, Glass Property Models and Constraints for Estimating the Glass to be Produced at Hanford by Implementing Current Advanced Glass Formulation Efforts, PNNL-22631 (2013).
- ²J. Matyáš, J.D. Vienna, A. Kimura, M. Schaible, and R.M. Tate, Development of Crystal-Tolerant Waste Glasses, *Ceramic Transactions* 222, 41-51 (2010).
- ³J. Matyáš, D.P. Jansik, A. T. Owen, C. A. Rodriguez, J. B. Lang, and A. A. Kruger, Impact of Particle Agglomeration on Accumulation Rates in the Glass Discharge Riser of the Melter, *Ceramic Transactions* 241, 59-68 (2013).
- ⁴R. E. Eibling, R. F. Schumacher, and E. K. Hansen, Development of Simulants to Support Mixing Tests for high Level Waste and Low Activity Waste, SRT-RPP-2003-00098 (2003).
- ⁵D. G. Rancourt and J. Y. Ping, Voight-Based Methods for Arbitrary-Shape Static Hyperfine Parameter Distributions in Mössbauer Spectroscopy, *Nucl. Instrum. Methods Phy Res Sect B* 58, 85-97 (1991).
- ⁶A. M. Gismelseed and A. A. Yousif, Mössbauer Study of Chromium-Substituted Nickel Ferrites, *Physica B* 370, 215-222 (2005).